

# Study on the Curing Reaction, Dielectric and Thermal Performances of Epoxy Impregnating Resin with Reactive Silicon Compounds as New Diluents

Yun Zheng,<sup>1,2</sup> Kim Chonung,<sup>1,2</sup> Xiaolin Jin,<sup>1,2</sup> Ping Wei,<sup>1,2</sup> Pingkai Jiang<sup>1,2</sup>

<sup>1</sup>School of Chemistry and Chemical Engineering, Shanghai Jiao Tong University, Shanghai 200240, People's Republic of China

<sup>2</sup>Shanghai Key Lab of Electric Insulation and Thermal Aging, Shanghai 200240, People's Republic of China

Received 10 July 2007; accepted 30 September 2007

DOI 10.1002/app.27502

Published online 26 November 2007 in Wiley InterScience (www.interscience.wiley.com).

**ABSTRACT:** Two silicon compounds including (3-glycid-oxypopyl)trimethoxysilane (A187) and (3-glycidoxypopyl)methyldiethoxysilane (W78) were used and studied as reactive diluents for aluminum (III) acetylacetonate (Alacac) accelerated epoxy/anhydride impregnating resin systems. The dielectric performances were studied and characterized by the dielectric dissipation factor, dielectric constant, volume resistivity, and breakdown strength. The curing behaviors and thermal properties of the cured impregnants were studied by Fourier transform infrared (FTIR) spectroscopy, differential scanning calorimetry (DSC), and thermogravimetry. The activation energies of different epoxy formulations

were determined with Kissinger method. The results showed that W78 was effective to decrease the viscosity and had little influence on the curing reaction. The cured sample of 15 parts-of-W78-containing-epoxy resin/methylhexahydrophthalic anhydride (MHHPA) accelerated by Alacac exhibits good dielectric and heat resistant performances with a dielectric dissipation factor below 0.04 at 155°C. © 2007 Wiley Periodicals, Inc. *J Appl Polym Sci* 107: 3127–3136, 2008

**Key words:** epoxy/anhydride; impregnating resin; dielectric properties; silicon compounds

## INTRODUCTION

At present, the vacuum pressure impregnation process (V.P.I.), especially the total (global) vacuum pressure impregnation process is one of the most promising technologies for the stator winding insulation of large electrical generators and motors. This technology has been widely studied and adopted by leading electrical equipment manufactures around the world.<sup>1–3</sup> The V.P.I. insulation system includes the impregnant, mica tape, equipments, and manufacturing techniques. Among these factors, the impregnant has a great influence on the insulation properties since it is one of the main components of the mica/epoxy composites as the insulating material for the stator winding insulation.

Epoxy resins are now considered to be the most preferable material for V.P.I technology because of their superior mechanical strength, chemical resistance, and electrical properties after cured by the an-

hydride hardeners. However, the viscosities of epoxy resins are usually high, which is not appropriate for the impregnating process at room temperature. To decrease the epoxy viscosity and to improve its processability, at least one reactive diluent should be employed in the impregnating resin formulations.

According to the studies by other authors,<sup>4,5</sup> the diluents used for epoxy impregnants may be divided into two varieties: the epoxy-based compounds and nonepoxy chemical compounds. In the case of epoxy-based compound, the presence of epoxide groups allows the crosslinking reaction of the diluents to occur at the same time that the epoxy resin is cured by the hardener. Most mono-epoxy diluents are excellent in reducing the viscosity, but cause a decrease in the crosslink density of the resin, resulting in serious impairment of other properties, especially its insulating properties. In the case of “polyfunctionality,” the behavior of the diluent is considered to be similar to that of the basic epoxy component and the crosslink density seems not to be affected. The disadvantage of such diluents is their relatively high viscosity, which is not efficient enough to satisfy the demand of the impregnating technology.

Typical diluents of nonepoxy chemical compounds are styrene and its derivatives; especially styrene is widely used in epoxy-ester impregnants. Those diluents are effective in reducing the epoxy viscosity.

Correspondence to: P. K. Jiang (pkjiang@sjtu.edu.cn) or Y. Zheng (carolzy@sjtu.edu.cn).

Contract grant sponsor: Shanghai Science and Technology Commission, China; contract grant number: 05dz22303.

*Journal of Applied Polymer Science*, Vol. 107, 3127–3136 (2008)  
© 2007 Wiley Periodicals, Inc.

But their high toxicity and latent danger to human body are unavoidable to the manufacturers and their customers.

Besides epoxy resin, reactive diluents and curing agent, one or more latent accelerators are also needed in the epoxy impregnating resin formulations. Various compounds including modified amine, imidazoles, organic tin, quaternary organic onium salts, and metal acetylacetonates (acacs) have been studied and used as latent accelerators for epoxy resin and anhydride curing systems.<sup>4,6,7</sup> It has been found that metal acacs are effective latent accelerators for anhydride-cured epoxy resins and have been widely studied and extensively used in recent years.<sup>8-10</sup> But their mechanism of acceleration has not been confirmed yet to our knowledge. Smith suggested that the decomposition products of the metal acacs might be the active species responsible for initiating polymerization in epoxy/anhydride resin systems.<sup>10</sup> Another study<sup>8</sup> considered that the metal acacs probably reacted with hexahydro-4-methylphthalic anhydride (HMPA) first to form a transition state that proceeded to cure the epoxy resins. The transition state of the reaction was considered to be both the breakage of the coordinate bond between the metal ion and acac and the establishment of the bond between acac and HMPA. In this study, Aluminum acetylacetonate (Alacac) is employed as the latent accelerator and its catalytic mechanism on the epoxy/anhydride curing reaction is characterized by heating-FTIR analysis.

The objective of this article is to study the effect of silicon compounds as reactive diluents on the curing reaction and performances of impregnating resin based on cycloaliphatic epoxy resin and methylhexahydrophthalic anhydride (MHHPA) system, catalyzed by aluminum (III) acetylacetonate (Alacac).

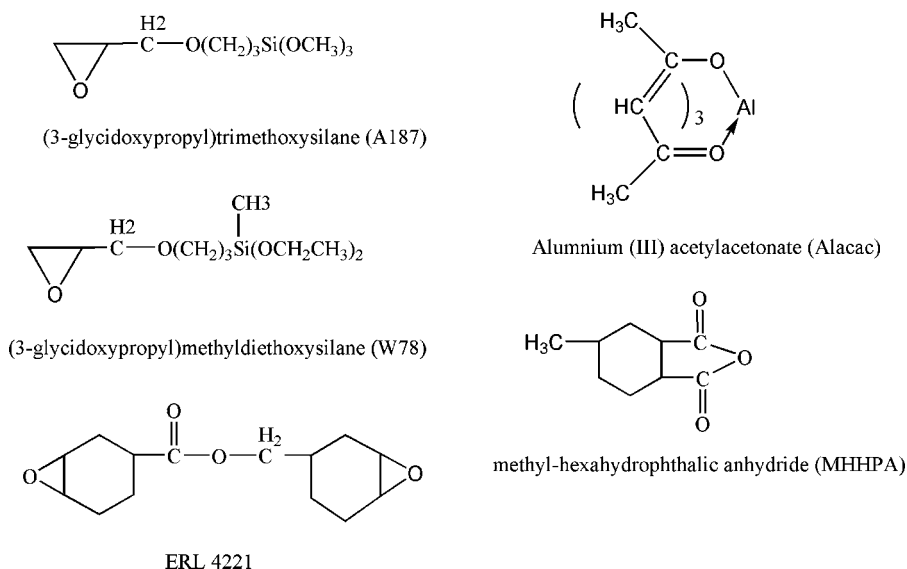
Two epoxy functional silanes with low degree of toxicity and low viscosity including (3-glycidoxypropyl) methyl-diethoxysilane and (3-glycidoxypropyl) trimethoxysilane used as reactive diluents are studied and compared.

## EXPERIMENTAL

### Materials and cure procedure

The epoxy resin used in this study was a kind of cycloaliphatic epoxy resins (Grade: ERL 4221, from Union Carbide Corp.) with an epoxy equivalent weight of 134–137 g/mol. The curing agent used in this study was MHHPA, purchased from Lon ca group, Italy. The molecular weight of MHHPA was 168 g/mol and its purity was >99%. Aluminum (III) acetylacetonate was used as the latent accelerator and purchased from Aldrich Chemicals, Inc. The silicon reactive diluents employed in this study were purchased from GE chemicals, including (3-glycidoxypropyl)methyl-diethoxysilane ( $C_{11}H_{24}O_4Si$ , molecular weight 248.39, toxicity (oral rat, LD50 >2000 mg/Kg), grade W78) and (3-glycidoxypropyl)trimethoxysilane ( $C_9H_{20}O_5Si$ , molecular weight 236.34, toxicity (oral rat, LD50) >8400 mg/Kg, grade A187). The chemical structures of the compounds employed in this study are presented in Scheme 1.

The samples were prepared according to the formulations listed in Table I. The required quantity of Alacac accelerator was first added to the epoxy resin, stirred at 80°C to obtain a homogeneous system in a three-necked flask. Then MHHPA and a diluent at designed ratios were added to this mixture, mixed vigorously, and then degassed in a vacuum oven at 60°C for about 30 min. The epoxy curing



**Scheme 1** Chemical structures of raw materials.

**TABLE I**  
**Formulations of Epoxy Impregnating Resin**

| Sample no. | The weight of different gradients (g) |       |     |      |        | Calculated mol ratio of epoxide and anhydride |
|------------|---------------------------------------|-------|-----|------|--------|---|
|            | ERL4221                               | MHHPA | W78 | A187 | Alacac |   |
| A          | 85                                    | 115   | 15  | 0    | 0.1    | 100/110                                       |
| B          | 85                                    | 106   | 15  | 0    | 0.1    | 100/100                                       |
| C          | 85                                    | 95    | 15  | 0    | 0.1    | 100/90  |
| D          | 85                                    | 85    | 15  | 0    | 0.1    | 100/80  |
| E          | 85                                    | 95    | 15  | 0    | 0.3    | 100/90  |
| F          | 85                                    | 95    | 15  | 0    | 0.5    | 100/90  |
| G          | 80                                    | 90    | 0   | 20   | 0.1    | 100/90  |
| H          | 85                                    | 95    | 0   | 15   | 0.1    | 100/90  |
| I          | 90                                    | 100   | 0   | 10   | 0.1    | 100/90  |
| J          | 85                                    | 95    | 0   | 15   | 0      | 100/90  |
| K          | 85                                    | 95    | 0   | 15   | 0.3    | 100/90  |
| L          | 100                                   | 110   | 0   | 0    | 0      | 100/90  |
| M          | 100                                   | 110   | 0   | 0    | 0.3    | 100/90  |
| N          | 85                                    | 73    | 15  | 0    | 0.1    | 100/70  |
| O          | 100                                   | 110   | 0   | 0    | 0.5    | 100/90  |
| P          | 100                                   | 0     | 0   | 0    | 0.5    | –   |
| Q          | 0                                     | 100   | 0   | 0    | 0.5    | –   |

systems were poured onto stainless steel plates, then precured in an oven at 135°C for 3 h, followed by a final cure at 150°C for 14 h.

### Characterization

#### Differential scanning calorimeter measurements

The calorimetric measurements were done on a Perkin-Elmer Pyris 1 differential scanning calorimeter (DSC) operating in a nitrogen atmosphere with a flow rate of 20 mL/min. The sample size was around 5 mg. The dynamic DSC analysis was performed in the temperature range between 20 and 300°C at five different heating rates of 5, 10, 15, 20, and 25°C/min.

#### TGA measurements

The thermo gravimetric analysis (TGA) were performed with a Perkin-Elmer 7 Series thermal analyzer at heating rate of 10°C/min under a nitrogen atmosphere with a flow rate of 20 mL/min, and the temperature ranged from room temperature to 800°C.

#### Morphology analysis

The morphology of the cured impregnants was observed with a field emission scanning electron microscopy (FE-SEM, JEOL JEM-4701, Tokyo, Japan).

#### Fourier transform infrared spectroscopy

Infrared spectral studies were performed on some of the resin formulations to elucidate the acceleration mechanism of Alacac. The spectra of liquid samples were obtained as smears on KBr plates using a

Perkin-Elmer 700 spectrophotometer. Solid samples were recorded as pressed KBr pellets.

#### Viscosity measurements

Viscosity measurements were made in the temperature range between 30 and 100°C using a rotational viscometer.

#### Dielectric performances

Dielectric performances including the dielectric dissipation factor ( $\tan \delta$ ), dielectric constant ( $\epsilon$ ), volume resistivity, and breakdown strength of the cured impregnants were obtained on sample discs with the diameter of 100 mm and the thickness of 1 mm. The dielectric dissipation factor ( $\tan \delta$ ) and dielectric constant ( $\epsilon$ ) data were obtained with Schering bridge (TETTEX AG Instrument, Switzerland) over the temperature range from 25 to 155°C at the frequency of 50 Hz. Breakdown strength data were obtained with alternating-current breakdown strength tester (AHDZ, Shanghai Lanpo) and volume resistivity data were tested with a digital high resistance meter (6517A, Keithley, USA).

## RESULTS AND DISCUSSION

### Influence of silicon compounds on the viscosity of epoxy resin

Containing one epoxy group in their molecular structure, W78 and A187 are mutually soluble with epoxy resin at all temperatures. The viscosity of W78 and A187 is very low (about 3 cps at 25°C), which makes them effective to reduce the viscosity of the

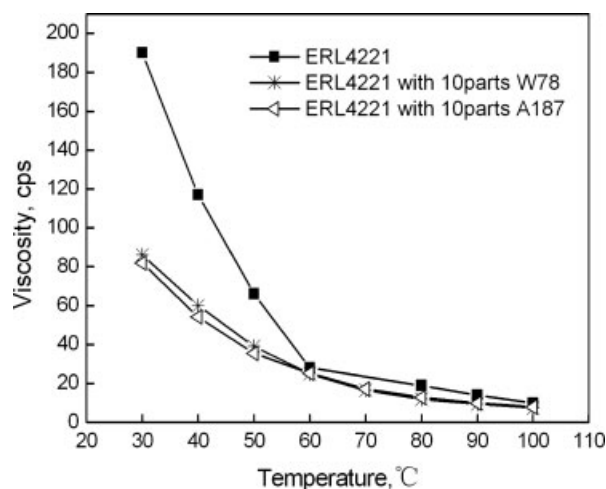


**Figure 1** The influence of silicon compounds on the viscosity of epoxy resin.

epoxy resin. Shown in Figure 1 are the plots of the epoxy viscosity versus temperature data. The reduction of original viscosity at 25°C has been found to be >50% when 10 parts of W78 or A187 were introduced into 100 parts of ERL4221 epoxy resin.

### Dielectric performances

The dielectric performances of samples cured with a variety of formulations (Table I) were tested and shown in Figure 2 and Table II.

Dielectric loss appears when an oscillating electric field is applied to a polar dielectric. There is a tendency of dipole molecules or parts of dipole molecules to rotate along the electric field overcoming the forces of internal friction of either the intermolecular interaction or the molecular friction, resulting in the expenditure of a part of electric energy and its conversion into thermal energy. All other conditions being equal, the greater the parameters of the electrical

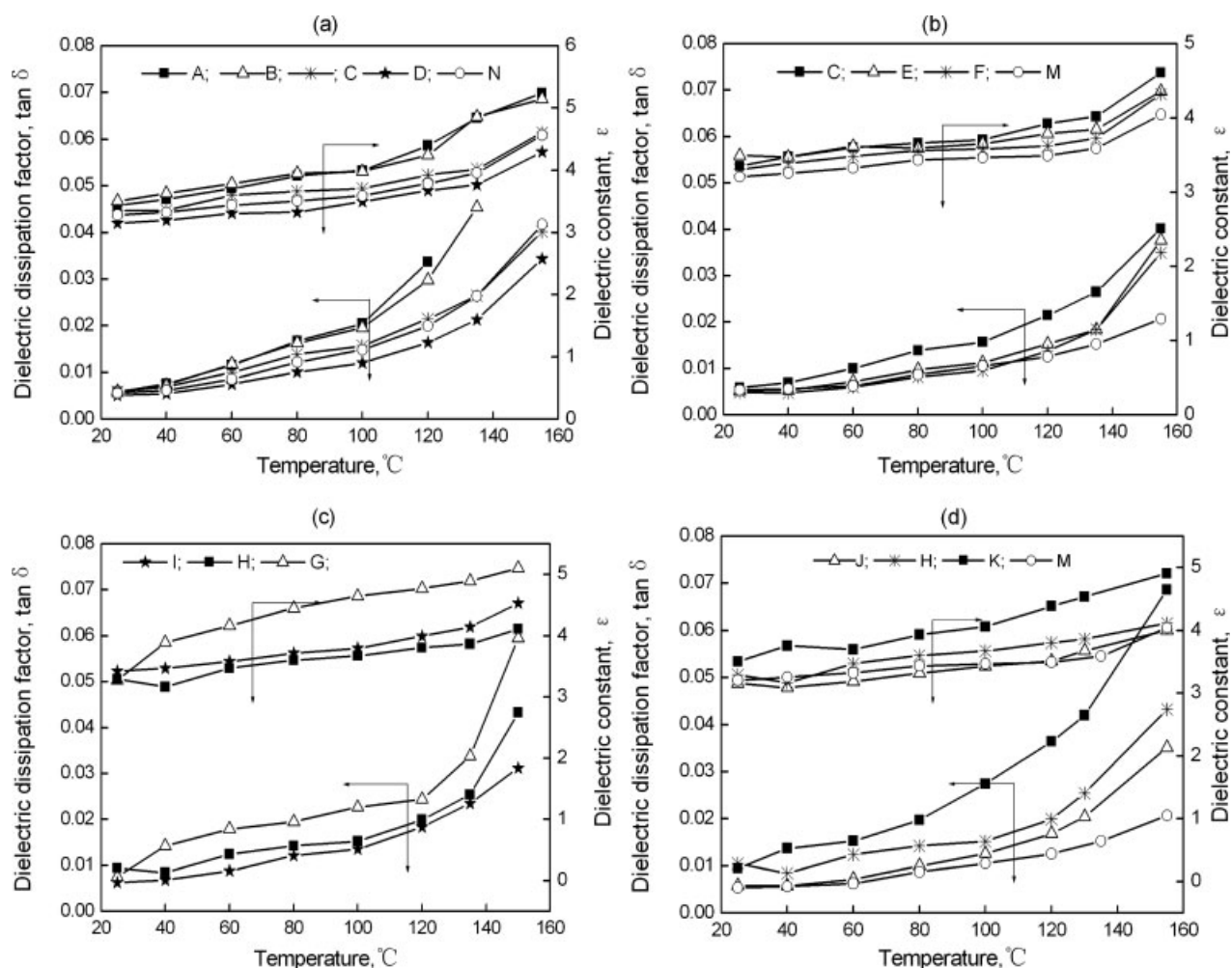


**Figure 2** The values of  $\tan \delta$  and  $\epsilon$  versus temperature for (a) the W78-containing-epoxy resin with different epoxide/anhydride ratio, (b) the W78-containing-epoxy resin with different Alacac concentrations, (c) the A187-containing-epoxy resin with different A187 concentrations, and (d) the A187-containing-epoxy resin with different Alacac concentrations.

**TABLE II**  
**Representative Dielectric Properties of Cured**  
**Impregnants With Different Diluents**

| Samples                                     | Sample M             | Sample E             | Sample K             |
|---|----------------------|----------------------|----------------------|
| tan $\delta$ , 25°C                         | 0.005                | 0.005                | 0.009                |
| tan $\delta$ , 155°C                        | 0.021                | 0.037                | 0.068                |
| $\epsilon$ , 25°C                           | 3.2                  | 3.5                  | 3.5                  |
| $\epsilon$ , 155°C                          | 4.1                  | 4.4                  | 4.9                  |
| Volume resistivity<br>( $\Omega$ cm, 25°C)  | $4.0 \times 10^{16}$ | $3.8 \times 10^{16}$ | $3.0 \times 10^{16}$ |
| Volume resistivity<br>( $\Omega$ cm, 155°C) | $1.2 \times 10^{16}$ | $7.5 \times 10^{15}$ | $3.9 \times 10^{14}$ |
| Breakdown strength<br>(KV/mm, 25°C)         | 34                   | 35                   | 30                   |

insulating material  $\epsilon$  and tan  $\delta$  are, the higher the dielectric losses become. The values of  $\epsilon$  and tan  $\delta$  differ with the chemical structure of different dielectrics and for given specimens of a material, they are not strictly constant and depend on various external factors like frequency, temperature, voltage, and humidity.<sup>11,12</sup> In this study, relationship of tan  $\delta$  and  $\epsilon$  with temperature at 50 Hz is discussed according to the application requirement in electrical generators.

Figure 2(a) shows the values of tan  $\delta$  and  $\epsilon$  versus temperature for the W78-containing-epoxy resin with different epoxide/anhydride ratio. Within 70–110 parts anhydride in per 100 parts epoxide, sample with the epoxide/anhydride ratio of 100/80 exhibits the lowest values of tan  $\delta$  and  $\epsilon$ . The decrease and increase of anhydride concentration both cause increase in the values of tan  $\delta$  and  $\epsilon$ . Samples with the epoxide/anhydride ratio of 100/70 and 100/90 exhibit similar dielectric performances with that of 100/80. This demonstrates that the stoichiometric proportion of the epoxy resin and MHPHA used in this study is around 100/80. During the curing process, epoxy resins react with anhydride via a ring-opening mechanism. The crosslinking occurs through the reaction of the terminal epoxy groups with anhydride groups, and subsequent reaction of epoxy groups with hydroxyl groups formed during the reaction. As the reaction goes on, epoxy and anhydride dipoles disappear, and some new dipoles, such as ester and hydroxyl groups, appear. In the crosslinked epoxy networks, the polarizability and mobility of the un-reacted residual dipoles and newly produced dipoles may account for the relaxational dielectric loss.<sup>13–16</sup> Therefore the epoxy/anhydride ratio should be stoichiometrically controlled; otherwise, excess epoxy or anhydride dipoles would exist in the crosslinked networks exerting double effect on dielectric loss. The first is that the excess epoxy or anhydride cause a “looser” network structure in which the dipoles or polar segments can rotate more easily along the electric field and the second is that the polarizability of excess epoxy or

anhydride dipoles are higher than that of the polar segments in the crosslinking epoxy network. As a result, dielectric loss will increase when too much or insufficient anhydride is used in the formulation. On the other hand, the MHPHA has very low viscosity, therefore, the more MHPHA in the epoxy resin formulation, the lower its viscosity and accordingly the better the processability. Considering the dielectric properties as well as the viscosity, the epoxide/anhydride ratio was modified to 100/90 in the following studies since there is no great difference in dielectric performances of the samples with epoxy/anhydride ratio between 100/80 and 100/90.

As presented in Figure 2(b), the W78-containing-epoxy resin with more Alacac shows lower values of tan  $\delta$  and  $\epsilon$ . This indicates higher conversion, cross-link degree, and more perfect crosslink structure, which constrain the dipoles more tightly to their places since there are no changes pertaining to the dipoles of the reaction system. It has been found that in the case of thermal or chemical treatment of polar organic dielectrics, which increases the extent of cure or polymerization, the dielectric dissipation loss tends to decrease and increase with temperature.<sup>11,16,17</sup> It's obvious that Alacac is effective to accelerate the curing reaction of epoxy resin with anhydride curing agent. However, there is no apparent difference between 0.3 parts and 0.5 parts of Alacac-accelerated impregnants, which means the employment of Alacac, can only improve the dielectric properties to a certain extent. Too much Alacac is found to be inappropriate since it shows no better influence on the dielectric properties. For the epoxy impregnants using W78 as a diluent, the proper Alacac concentration should be 0.10–0.50 parts. It can also be observed from Figure 2(b) that there are no obvious differences in the values of tan  $\delta$  and  $\epsilon$  for sample E and M at temperatures lower than 135°C. The incorporation of 15 parts of W78 causes an increase in the values of tan  $\delta$  at 155°C. The increase in dielectric loss should be determined by the structures of the W78 compound, which is aliphatic and mono-epoxide functionalized rather than alicyclic and double-epoxide functionalized. This may cause decrease in the cross-link density which results in decreased bondage on the activity of dipoles and ions at high temperature.

When considering the temperature dependence of the dielectric index, the values of tan  $\delta$  and  $\epsilon$  increase gradually with the temperature increment at low temperature range, e.g., at temperatures lower than 135°C in Figure 2(b). At high temperature range, e.g., at temperatures higher than 135°C in Figure 2(b), the values of tan  $\delta$  increase more quickly with the increasing of the temperature. It has also been found that the cured impregnant with a lower value of tan  $\delta$  generally exhibits a lower value of  $\epsilon$ . These indicate that apart from relaxational polarization,

ionic conductivity is also related to the appearance of dielectric losses. The peak of relaxational dielectric loss related to the segmental motion is difficult to distinguish, especially at low frequencies and is not observed in our study. This may be because of the strong contribution of ionic conductivity which increases greatly at elevated temperatures.<sup>14,15,18</sup> At low temperature range, the dipoles and the ionic particles are constrained tightly in their places and their motions are "frozen." Therefore, the dielectric loss is low. With the increasing of the temperature, the motions of the dipoles and ionic impurities are activated. The elevation of temperature also increases the dissociation of weak linkage to ions. Accordingly, the dielectric loss increases.

The values of  $\tan \delta$  and  $\epsilon$  for the A187-containing-epoxy resin with different A187 concentrations are given in Figure 2(c). It can be observed that the values of  $\tan \delta$  for the cured sample increase with the increasing of A187 concentration. And there is no serious deterioration in the dielectric performances of samples containing no more than 15 parts of A187 when 0.1 parts of Alacac catalyst is used. Shown in Figure 2(d) are the values of  $\tan \delta$  and  $\epsilon$  versus temperature for the A187-containing-epoxy resin with different Alacac concentration. The dielectric data for the epoxy resin without diluent (sample M) is also given in Figure 2(d) for easy comparison. It is obviously shown that the sample K exhibits greatly increased dielectric loss than the sample M in the whole test temperature range, which indicates that with the catalysis of 0.3 parts Alacac, the incorporation of 15 parts of A187 in the epoxy resin causes great increase in dielectric loss. This result also indicates that comparing with W78, the incorporation of A187 into the epoxy resin results in more decrease in both the insulating properties at high temperature

and the heat resistance, which will be proved later in the following TGA analysis. It has also been found from Figure 2(d) that in contrast to W78, the dielectric data for the A187-containing-epoxy resin increase with the increasing of Alacac concentration. Sample without Alacac catalyst (sample J) shows the lowest values of  $\tan \delta$  and  $\epsilon$  which are a little higher than those of sample M. These results imply that secondary reactions besides epoxide and anhydride polymerization may be catalyzed by Alacac during the curing process in the A187-containing-epoxy impregnant. The complicate curing reaction will be characterized in the following DSC analysis.

The representative dielectric performances for sample M, E and K are listed in Table II. In comparison, the incorporation of W78 in the epoxy impregnant results in slight decrease in the dielectric performances. The great decrease of dielectric performances for the A187-containing-epoxy impregnant with the catalysis of Alacac implies a lower crosslinking degree or defects in the crosslinking structures. This should be related to the complicate reaction of the A187-containing-epoxy resin.

#### Analysis of thermal stability

The thermal degradation behavior and thermal stability of the cured impregnants were investigated by TGA under a nitrogen atmosphere. The TGA thermograms for the cured impregnants are shown in Figure 3(a,b). The TGA data including the maximum decomposition rate temperature, temperatures at characteristic weight losses (5, 10, 20, 30, and 50%) and residual weights at characteristic temperatures (300, 400, and 500°C) are summarized in Table III.

In the cases of the W78-containing-epoxy resin (sample E) and no diluent system (sample M), no

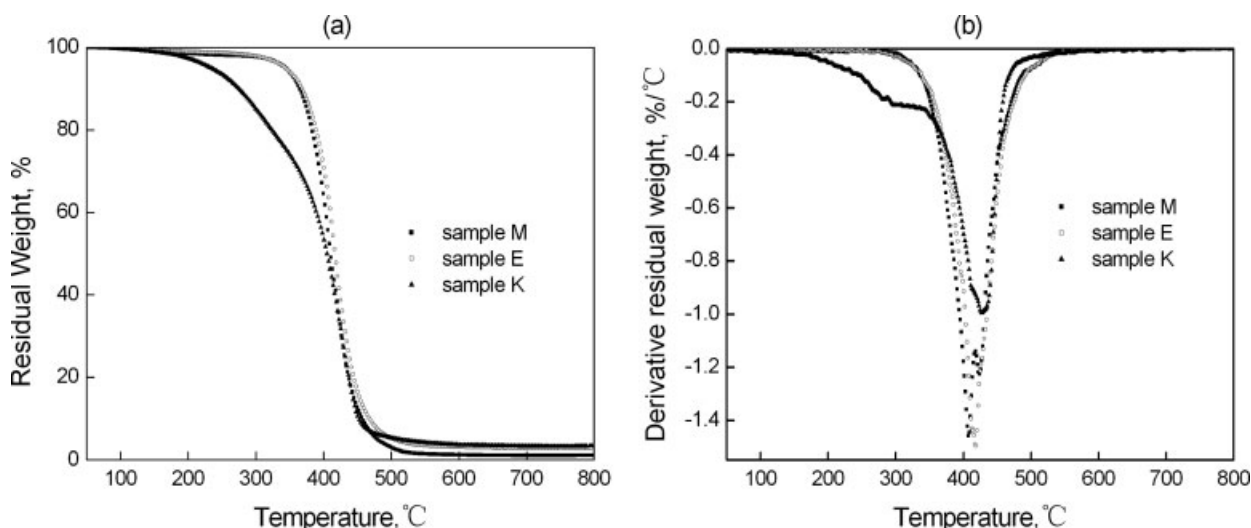


**Figure 3** TGA thermograms for the cured impregnants under a nitrogen atmosphere (a) residual weight versus temperature, and (b) derivative residual weight versus temperature.

**TABLE III**  
**TGA Data of Cured Epoxy Impregnants in Nitrogen Environment**

| Sample no. | $T_{\max}$ | Temperature at characteristic weight loss ( $^{\circ}\text{C}$ ) |       |       |       |       | Residual weight (%)    |                        |                        |
|------------|------------|--|-------|-------|-------|-------|------------------------|------------------------|------------------------|
|            |            | 5%   | 10%   | 20%   | 30%   | 50%   | 300 $^{\circ}\text{C}$ | 400 $^{\circ}\text{C}$ | 500 $^{\circ}\text{C}$ |
| M          | 408.1      | 344.0  | 365.0 | 383.2 | 395.0 | 410.8 | 97.7                   | 63.7                   | 3.1                    |
| E          | 418.2      | 344.2  | 368.7 | 389.2 | 402.0 | 417.5 | 97.9                   | 71.5                   | 8.3                    |
| K          | 426.9      | 234.7  | 275.5 | 324.2 | 364.7 | 405.2 | 85.0                   | 53.4                   | 5.4                    |

$T_{\max}$ , maximum decomposition rate temperature.

significant weight loss is observed up to 300 $^{\circ}\text{C}$ . And a one-stage decomposition process with  $T_{5\%}$  of about 344 $^{\circ}\text{C}$  was observed for the both samples heated in nitrogen. This weight loss may be considered to come from the decomposition of the epoxy matrix. The A187-containing-epoxy resin (sample K) shows relatively poorer temperature stability than the other two systems because obvious weight loss at temperatures below 300 $^{\circ}\text{C}$  is observed. It exhibits a two-stage decomposition process and the first-stage decomposition occurs at a much lower temperature (5% weight loss at 234 $^{\circ}\text{C}$ ). The first stage of weight loss at a lower temperature may come from the decomposition or the volatilization of some low molecular weight compounds produced during the curing process, and the second-stage weight loss from the decomposition of the resin matrix.

It can be clearly seen from Table III that sample E exhibits the best temperature stability, since the temperatures corresponding to all of the listed characteristic weight losses are the highest and the residual weights at the listed characteristic temperatures are the largest. The temperature stability of sample M is similar to that of sample E, whereas sample K shows poorer temperature stability. This gives some explanations as to why the cured A187-containing-epoxy resin shows decreased dielectric performances at

high temperatures. It can be deduced from the above experimental results that some byproducts with small molecular weights may be produced and embedded in the epoxy crosslinking network during the curing process of A187-containing-epoxy resin/MHHPA/Alacac systems. The motions of the byproducts with small molecular weight can be considered to be tightly constrained at room temperature, while with the increase of temperature their motions are released resulting in high dielectric losses.

#### Microstructure analysis of the cured epoxy impregnants

Shown in Figure 4 are the SEM micrographs of the fractured surfaces frozen under cryogenic condition using liquid nitrogen for the W78-containing-epoxy resin (sample E) and the A187-containing-epoxy resin (sample K). Referring to the micrograph (a), the fracture paths for the W78-containing-epoxy resin are broad, branched and discontinuous. The fracture surface is smooth with low ridges and shallow grooves and no phase separation is observed. The micrograph of the A187-containing-epoxy resin (b) exhibits narrow and continuous fracture paths indicating rapid crack propagation along the axis of crack growth. The morphology is indicative of brittle

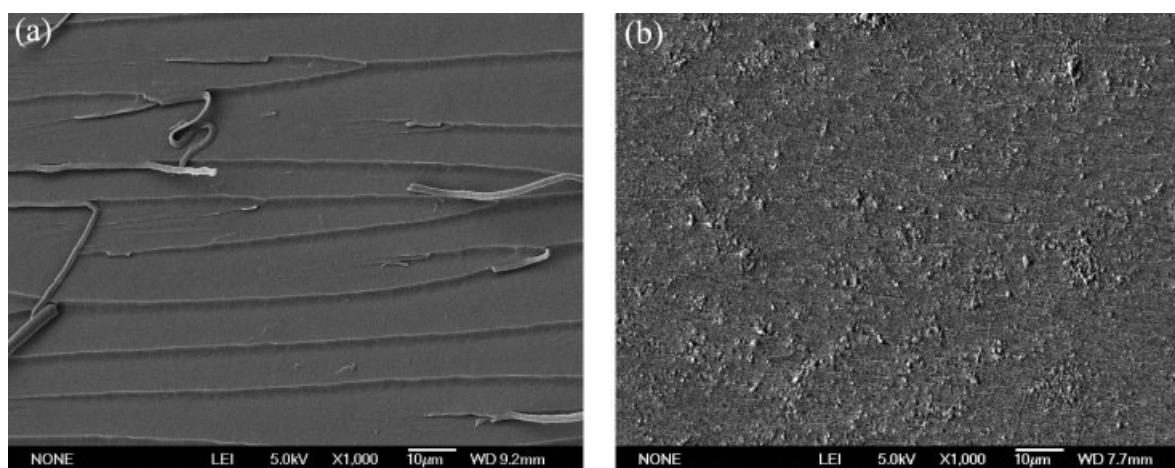


**Figure 4** SEM micrographs of the fractured surfaces for (a) the W78-containing-epoxy resin, and (b) the A187-containing-epoxy resin.

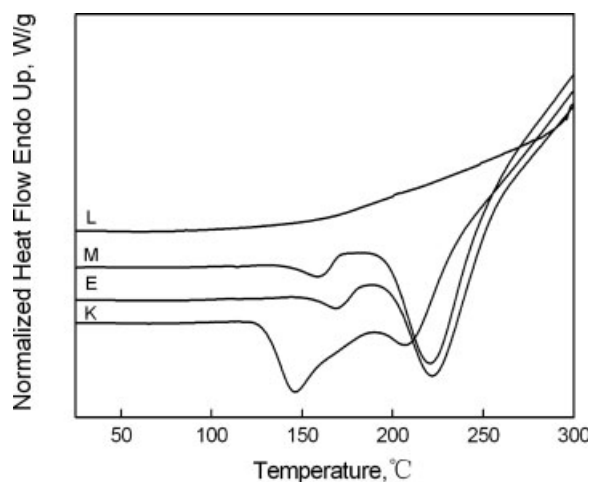


**Figure 5** Dynamic DSC curves for selected systems at a heating rate of 10°C/min.

fracture and particles with irregular shapes and sizes are observed on the fractured surface, which demonstrates inhomogeneity in the microstructure. The SEM morphological fractures are in good agreement with the trend in dielectric properties for epoxy resins containing different diluents.

#### Analysis of DSC data

Dynamic DSC measurements were performed to understand different influences of silicon diluents on the curing reaction of the epoxy/MHHPA system. Shown in Figure 5 are the DSC curves for different ERL4221/MHHPA/Alacac/diluent formulations. The formulations (L, M, E, and K) are listed in Table I. The samples according to different formulations were prepared as the method mentioned in the experimental section. About 5 mg of each sample was enclosed in aluminum pans, introduced to the calorimeter and heated from 20 to 300°C at a heating rate of 10°C/min. In the mixture of pure ERL4221 and MHHPA (sample L), epoxide and anhydride can be considered to react slowly during the heating procedure since no sharp exothermic peak is observed in the DSC plot. Two separated exothermic peaks are observed when Alacac is added to the ERL4221 and MHHPA mixture (sample M), one weak peak at a lower temperature and a very strong one at a higher temperature, which indicates the remarkable accelerating effect of Alacac on the reaction of epoxide and anhydride. The shape of the nonisothermal DSC curve for the W78-containing-epoxy resin (sample E) is very similar to that of sample M. Differently, two broad and overlapped exothermic peaks are observed in the case of the A187-containing-epoxy resin (sample K). This indicates that two different kinds of reaction may occur during the curing procedure: One reaction could be the hydrolysis

and condensation reaction of methoxysilane groups which is accelerated by Alacac, and the other reaction occurring at a higher temperature may be the esterification of epoxide with anhydride catalyzed by Alacac. The hydrolysis and condensation of methoxysilanes at lower temperatures causes such a sharp increase in viscosity that the later curing polymerization of epoxide and anhydride may be seriously hindered. Ethoxysilane is not as active as methoxysilane that the hydrolysis and condensation reaction can not be observed at lower temperature in sample E.

It is also found that in the case of sample E the DSC curve shows a slight increase at the temperature corresponding to the curing peaks, indicating a slight decrease in the reaction rate of the system. In contrast, in the case of sample K, the DSC curve shows a decrease at the temperature corresponding to the location of the curing peaks, indicating an increase in the reaction rate of the system.

The kinetic parameters for the curing reaction can be evaluated according to Kissinger's approach, which assumes that the maximum reaction rate occurs at the peak temperature.<sup>19–21</sup> It can be expressed as

$$\ln(\beta/T_p^2) = \ln(AR/E_a) + (-E_a/RT_p) \quad (1)$$

Where  $\beta$  is the linear heating rate,  $T_p$  is the temperature of the peak exothermic cure,  $A$  is a pre-exponential constant, and  $R$  is the universal gas constant. Therefore, the plot of  $\ln(\beta/T_p^2)$  versus  $1/T_p$  give the values of  $E$  and  $A$ .

DSC temperature scans were performed on the catalyzed epoxy resin systems (sample M, E, and K) with heating rates of 5, 10, 15, 20, and 25°C/min. The plots of the Kissinger equations are shown in Figure 6. Two Kissinger plots and activation energies have been determined in our case according to two

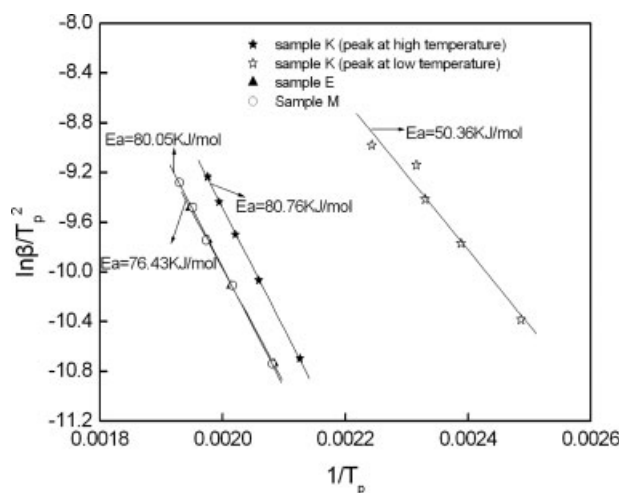


**Figure 6** Kissinger plots for selected epoxy impregnating systems.



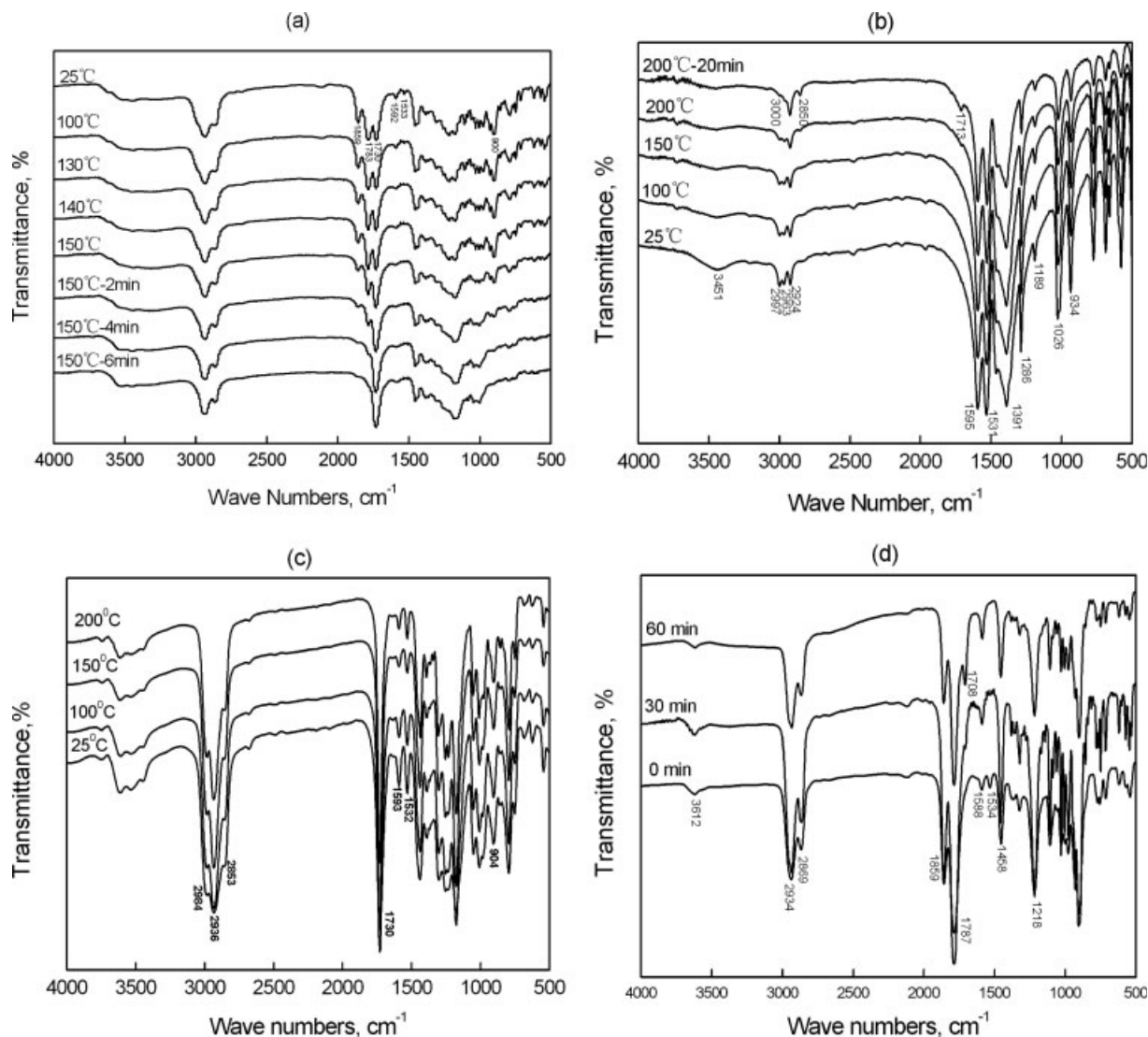
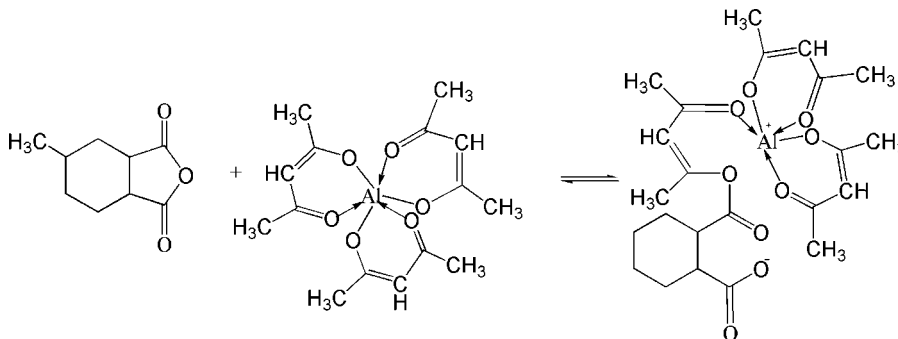


**Figure 7** FTIR spectra for (a) ERL4221/MHHPA/Alacac mixture, (b) MHHPA and Alacac mixture, (c) Alacac and (d) ERL4221 and Alacac Mixture, respectively.

strong and overlapped exothermic peaks observed in the dynamic DSC curves of sample K. They may be related to the hydrolysis and condensation of methoxysilanes and the esterification of epoxide and anhydride respectively.

#### Analysis of Alacac accelerating mechanism on curing reaction

Heating FTIR was used to characterize the reaction between epoxide, anhydride and Alacac. The FTIR results are illustrated in Figure 7. The assignments of the



**Scheme 2** The reaction of MHHPA and Alacac.

absorption features are as follows<sup>20,22,23</sup>: 3700  $\text{cm}^{-1}$  – 3320  $\text{cm}^{-1}$  to the hydroxyl groups, 3000  $\text{cm}^{-1}$  – 2850  $\text{cm}^{-1}$  to the C–H bond, 1860 and 1785  $\text{cm}^{-1}$  to the anhydride C=O, 1700  $\text{cm}^{-1}$  to the carboxylic anion C=O, 1731  $\text{cm}^{-1}$  to the ester linkage C=O, 1590 and 1533  $\text{cm}^{-1}$  to the chelated C=O, 900  $\text{cm}^{-1}$  to the epoxy groups.

The mixture of ERL4221/MHHPA/Alacac (sample O) was coated on a KBr plate, heated from 25 to 150°C at the heating rate of 10°C/min and held at 150°C for 30 min. The recorded FTIR spectra are shown in Figure 7(a). It is found from Figure 7(a) that the stretch absorption bands for C=O in anhydride (1850 and 1780  $\text{cm}^{-1}$ ) and C–O–C in epoxide (900  $\text{cm}^{-1}$ ) disappeared completely after several minutes at 150°C. Correspondingly, the absorption intensity at 1730  $\text{cm}^{-1}$  for the C=O in the newly formed ester linkage becomes stronger. All these changes indicate that the main reaction of curing is likely to be an esterification reaction. At the same time one (1533  $\text{cm}^{-1}$ ) of the characteristic absorption bands (1592 and 1533  $\text{cm}^{-1}$ ) of the chelated C=O is observed to disappear, which shows that the coordinate bonds may be broken.

Alacac and its mixture with ERL4221 (sample P) were heated from 25 to 200°C at the heating rate of 10°C/min and kept at 200°C for 30 min. The recorded FTIR spectra are shown in Figure 7(b,c), respectively. No obvious changes of the absorption bands are observed in the temperature range from 25 to 200°C. Changes of stretch absorption of C–H (2850–3000  $\text{cm}^{-1}$ ) and appearance of C=O in carboxylic anion (1713  $\text{cm}^{-1}$ ) are observed in the FTIR spectrum of Alacac after kept at 200°C for 20 min. This may be attributed to the decomposition of Alacac. To avoid water absorption, the mixture of Alacac and MHHPA (sample Q) was heated under a magnesium light lamp and the FTIR spectra obtained at different time are shown in Figure 7(d). It is observed that the absorption band at 1534  $\text{cm}^{-1}$  for chelated C=O in Alacac has disappeared and new absorption band at 1708  $\text{cm}^{-1}$  appeared after heating, which may indicate the formation of carboxylic anion structure in MHHPA and Alacac mixture.

From these heating FTIR studies, the catalytic mechanism of Alacac in the curing reaction of epoxide and anhydride can be considered to be that MHHPA first reacts with Alacac to form a carboxylic anion as a transition state at elevated temperatures (as shown in Scheme 2), then the carboxylic anions interact with the epoxide groups to initiate the curing reaction.

## CONCLUSIONS

The influences of the silicon compounds A187 and W78 on the performances and the curing reaction of

Alacac-accelerated epoxy/MHHPA impregnating resin systems have been investigated. The results indicate that the reactivity of the diluent has great influence on the morphology and network structure of the cured epoxy resin and thereby the dielectric and thermal performances. It is found that W78 is appropriate as a reactive diluent since it has little influence on the curing reaction and does slight impairment to the dielectric and thermal performances of the cured epoxy impregnating resin. While in the case of the A187-containing-epoxy resin especially with the catalysis of Alacac, the polymerization of epoxy and MHHPA is hindered by the hydrolysis and condensation of trimethoxysilane which result in low crosslink degree. Consequently, the A187-containing-epoxy resin exhibits poor dielectric performances and thermal stability. According to the heating FTIR analysis we found that the catalytic mechanism of Alacac in the curing reaction of epoxide and anhydride is that Alacac can react with MHHPA to form a carboxylic anion as a transition state which interacts with the epoxide groups to initiate the curing reaction.

## References

1. Chabra, O. P.; Kumar, M. C. Conference Record of the 2000 IEEE International Symposium on Electrical Insulation, 2–5 April, 2000.
2. Boulter, E. A.; Stone, G. C. *Electrical Insulation Magazine*, IEEE 2004, 20, 25.
3. Frost, N. E.; Hughes, D.; Laurenty, D.; Miller, G. H.; Isola, V. R. *Electrical Insulation Conference and Electrical Manufacturing & Coil Winding Technology Conference 2003*, Proceedings, 23–25 Sept, 2003.
4. Smith, J. D. B. *Electrical Electronics Insulation Conference 1995*, and *Electrical Manufacturing & Coil Winding Conference*, Proceedings 18–21 Sept, 1995.
5. May, C. A.; Nixon, A. C. *J Chem Eng Data* 1961, 6, 290.
6. Miyashiro, J. J.; Seiling, A. W. U.S. Pat. 3,624,032 (1969).
7. Smith, J. D. B.; Kauffman, R. N. U.S. Pat. 4,026,862 (1974).
8. Zhang, Z. Q.; Wong, C. P. *J Appl Polym Sci* 2002, 86, 1572.
9. Mark, M.; Schenectady, N. Y. U.S. Pat. 3,812,214 (1974).
10. Smith, J. D. B. *J Appl Polym Sci* 1981, 26, 1979.
11. Tareev, B. W. *Physics of Dielectric Materials*, Translated from the Russian by A. Troitsky, Mir Pub: Moscow, 1975; Chapter 3.
12. Sheu, E. Y.; Acevedo, S. *Fuel* 2006, 85, 1953.
13. Zong, L. M.; Zhou, S. J.; Sgriccia, N.; Hawley, M. C. *Polym Eng Sci* 2005, 45, 1576.
14. Soares, B. G.; Leyva, M. E.; Moreira, V. X.; Barcia, F. L.; Khastgir, D.; Simao, R. A. *J Polym Sci Part B: Polym Phys* 2004, 42, 4053.
15. Andjelic, S.; Mijovic, J. *Macromolecules* 1998, 31, 8463.
16. Zong, L. M.; Kempel, L. C.; Hawley, M. C. *Polymer* 2005, 46, 2638.
17. Saito, S. *Colloid Polym Sci* 1963, 189, 1435.
18. Sun, Y. Y.; Zhang, Z. Q.; Moon, K. S.; Wong, C. P. *J Polym Sci Part B: Polym Phys* 2004, 42, 3849.
19. Kissinger, H. E. *Anal Chem* 1957, 29, 1702.
20. Bai, L. B.; Liu, Y. H. *J Appl Polym Sci* 2007, 103, 2376.
21. Gonis, J.; Simon, G. P.; Cook, W. D. *J Appl Polym Sci* 1999, 72, 1479.
22. Dureault, V. O.; Gosse, B. *J Appl Polym Sci* 1998, 70, 1221.
23. Sun, G.; Sun, H. G.; Liu, Y.; Zhao, B. Y.; Zhu, N.; Hu, K. *Polymer* 2007, 48, 330.